

**GT2011-45(+)**

**UNSTEADY FLOW ANALYSIS OF INTERACTION BETWEEN JET-WAKE FLOW  
AND BLADES OF LOW SOLIDITY CASCADE DIFFUSER IN A CENTRIFUGAL BLOWER**

Daisaku Sakaguchi  
Faculty of Engineering  
Nagasaki University, Japan  
daisaku@nagasaki-u.ac.jp

Tengen Murakami  
Graduate School of Science and Technology  
Nagasaki University, Japan  
tengen@tfl.mech.nagasaki-u.ac.jp

Hironobu Ueki  
Graduate School of Science and Technology  
Nagasaki University, Japan  
ueki@nagasaki-u.ac.jp

Masahiro Ishida  
Professor Emeritus, Nagasaki University, Japan  
hiro@nagasaki-u.ac.jp

Hiroshi Hayami  
ASME Fellow  
Professor Emeritus, Kyushu University, Japan  
hayami@cm.kyushu-u.ac.jp

*Key Words:* Centrifugal blower, Low solidity cascade diffuser, Secondary flow, Shroud tip-groove

**ABSTRACT**

A low solidity cascade diffuser (LSD) shows features of a wide operating range and a high pressure ratio in centrifugal compressors and blowers. According to the steady flow analysis results shown previously by the authors, the noise could be reduced effectively without deterioration of the LSD performance by means of a small blade tip-groove located at the shroud side, and a high blade loading could be achieved without stall even at the angle of attack as large as 15 deg. The high LSD performance at low flow rates was achieved by both formations of the stable and intense vortex in the shroud tip-groove and of the secondary flow moving circumferentially along the shroud wall toward the impeller exit. In the present study, the influence of the rotating jet-wake flow discharged from the impeller on the vortex in the shroud tip-groove and on the secondary flow moving circumferentially along the shroud wall were investigated by comparing the simulation results between the unsteady flow analysis and the steady flow one. It is clearly shown that the lift force of the LSD blade fluctuates periodically with the blade passing frequency, however, the flow behaviors of the vortex in the shroud tip-groove and the secondary flow on the shroud wall are little affected by the rotating jet-wake in the vaneless space.

**INTRODUCTION**

A high pressure ratio and a wide operating range are required in recent centrifugal compressors and blowers, however, it is generally difficult to achieve both of a high pressure ratio and a wide operating range simultaneously. In order to improve the performance, it is essential to understand an interaction between the rotating impeller blade and the stationary diffuser blade, then, many studies have been conducted on rotor-stator interaction experimentally and numerically. Kang et al. [1] measured and analyzed the unsteady pressure fluctuation in the channel diffuser of a centrifugal compressor. According to their results, a periodic fluctuation due to blade passing did not decay in the diffuser channel, however aperiodic fluctuation decreased rapidly downstream of the diffuser channel. Liu et al. [2] investigated the unsteady rotor-stator interaction in a transonic centrifugal compressor with vaned diffuser by the numerical simulation. They found the circumferential flow variation and its unsteadiness at the impeller exit affected significantly on the diffuser performance. Anish et al. [3] analyzed numerically centrifugal compressor performances under various rotor-stator interactions. Based on the transient simulation, it was found that the loading of the diffuser vane and the diffuser static pressure recovery were

affected by the rotating jet-wake flow.

Senoo et al. [4] proposed the low-solidity circular cascade diffuser (LSD) firstly to achieve a wide flow range as well as a high efficiency for a low-speed centrifugal blower. Hayami et al. [5,6] developed further the LSD for a transonic centrifugal compressor and the effectiveness of the LSD was demonstrated experimentally at several different rotational speeds. The LSD showed the higher diffuser performance and the wider operating range as well as every rotational speed in comparison with the vaneless diffuser. Bonaiuti et al. [7] investigated the internal flow of the LSD for the transonic diffuser by the numerical simulation. The secondary flow was investigated in detail and the unsteady numerical results showed that a high level of unsteadiness was associated with the recirculating zone at the stall flow rate.

Another technical issue for the LSD is noise. It has been found that the typical discrete frequency noise increases due to the interaction between the impeller and the stationary diffuser blades. The authors [8] studied the effect of the LSD blade leading edge location on the diffuser performance and the sound pressure level experimentally in a centrifugal blower. It was found that the increase in noise due to LSD is dependent mainly on the broadband noise and secondarily on some kinds of discrete frequency noise. The typical discrete frequency noise corresponding to the blade passing frequency (BPF) is due to the jet-wake flow and the potential interaction between the rotating impeller blade and the LSD blade. The broadband noise increases with the lift force of the LSD blade, then, the noise increase due to the LSD seems to be mainly caused by the pressure fluctuation induced by the vortex shedding from the LSD blade. In this case, the noise was decreased without deterioration of the diffuser performance by locating the LSD leading edge at  $R_{LSD} = 1.20$  where the jet-wake flow is almost completely uniformized. [9]

Similar studies on interaction noise radiated from a centrifugal compressor with a vaned diffuser, and improvement of surge margin as well, were conducted by Goto et al. [10] and Zhang et al. [11]. They adopted the tapered diffuser vanes and showed that it was effective for reduction of interaction noise because of the smaller interaction area between impeller-discharge flow and diffuser vane surface. The optimized hub-side tapered diffuser vane shown by Ohta et al. [12] could suppress the evolution of the leading-edge vortex and resulted in improvement of compressor performance at low flow rates. The authors [13] also found that the noise could be reduced effectively without deterioration of the LSD performance by means of a small blade tip-groove located at the shroud side, and high blade loading could be achieved without stall even at the angle of attack as large as 15 deg. The formations of the stable and intense vortex in the shroud tip-groove and the secondary flow moving circumferentially along the shroud wall toward the impeller exit were the key factors for achieving a

high LSD performance at low flow rates.

The objective of the present study is to clarify the effect of the jet-wake flow on the formation of vortex in the tip-groove and on the secondary flow moving circumferentially on the diffuser wall. In order to simulate the jet-wake flow from the rotating impeller, the unsteady flow analysis was performed in the calculation domains with all impeller passages and all LSD passages. The unsteady flow in the LSD was analyzed in the view point of unsteadiness of flow separation, lift fluctuation and the vortex in the shroud tip-groove.

## NOMENCLATURE

$b$	: Diffuser depth [mm]
$C_{PR}$	: Pressure recovery coefficient ( $=2(p-p_2)/(\rho V_2^2)$ )
$C_L$	: Lift coefficient ( $=2L/(\rho V^2 b l)$ )
$L$	: Lift force [N]
$l$	: Chord length [mm]
$p$	: Static pressure [Pa]
$P_0$	: Total pressure in suction plenum tank [Pa]
$Q$	: Discharged flow rate [m <sup>3</sup> /s]
$r$	: Radius [mm]
$R$	: Radius ratio ( $=r/r_2$ )
$R_{groove}$	: Radius ratio of tip-groove rear edge
$T$	: Time interval passing one pitch of impeller blade
$U_2$	: Impeller tip speed [m/s]
$V$	: Absolute flow velocity [m/s]
$\alpha$	: Angle of attack [deg]
$\phi$	: Flow coefficient ( $=Q/2\pi r_2 b_2 U_2$ )
$\psi_s$	: Static pressure coefficient ( $=2(p-P_0)/\rho U_2^2$ )
$\rho$	: Density of fluid [kg/m <sup>3</sup> ]

## Subscript

2	: Impeller exit
e	: Diffuser exit
d	: Diffuser

## EXPERIMENT AND NUMERICAL SIMULATION

The test facility was specially designed to keep axisymmetrical flow field in the present research work. The test impeller was a low specific speed type unshrouded centrifugal impeller for industrial use, and it has the exit diameter of 510 mm and 16 backward leaning blades with the exit blade angle of 45 deg. The exit blade height is 17.0 mm, and the axial clearance between the impeller shroud tip and the shroud casing is 1.0 mm. The air was discharged axisymmetrically to the atmosphere from the diffuser exit with its radius ratio of about 1.6 as shown in Fig.1. Figure 2 also shows the location and shape of the LSD blade with small tip-grooves near the leading edge. The LSD blade was the U.S.A. 35-B airfoil and the chord length was 121 mm. The number of the LSD

blade was 11 and the solidity of the cascade was 0.693. The LSD blade leading edge was located at the radius ratio of  $R=1.10$  downstream of the impeller exit, and the tip-groove configuration is shown by the gray portion between  $R=1.10$  and 1.14. In spanwise, the tip-groove was located only at the shroud side with 2 mm height. The stagger angle of the LSD blade was fixed at 66 deg, which was equal to the average absolute flow angle discharged from the impeller at the design flow rate of  $\phi_d=0.27$ . In the experimental study, the impeller was operated at a constant speed of  $2,000\pm 2$  rpm. The static pressures were measured by means of manometer at the suction plenum tank located upstream of the suction pipe and at the impeller exit,  $R=1.0$  on the shroud wall. The flow rate was measured by using the entrance nozzle at the inlet of suction pipe. Noise was measured by means of the 1/2 inch condenser microphone (B&K 4189) with a windscreen, which was located at 100 mm downstream from the diffuser exit. The sound pressure spectra were analyzed by using the real-time FFT analyzer (CF-5210) produced by ONO SOKKI Co. Ltd.

The 3-D turbulent internal flow was calculated by using the commercial CFD code of ANSYS-CFX12 together with the baseline  $k-\omega$  turbulence model. The multi-frame of references consisting of the rotating domain of the impeller section and the stationary domain of the diffuser section were adopted. In the steady flow analysis, one of the impeller passages and one of the LSD passages were selected and the periodic boundary condition was applied at the mid-pitch of the blade passage. The grid number is about 150,000 for the rotating domain and about 320,000 for the stationary domain. At the LSD blade surface, the area averaged  $y^+$  was 7.6 and 1.4 in the cases with and without the shroud tip-groove respectively. The domain interface between the rotating frame and the stationary frame was located at  $R=1.01$  in the vaneless space, and the circumferentially averaged values were distributed pitch-wise on the domain interface. Then, non-uniformity of the circumferential flow distortion at the upstream exit boundary was not retained at the downstream inlet boundary although the flow distortion in the meridional plane was conserved at the interface. On the other hand, in the unsteady flow analysis, calculation domains are all impeller passages and all LSD passages respectively. Figure 3 shows the computational grid for the unsteady simulation. The grid number is about 300,000 for the rotating domain and about 700,000 for the stationary domain. The domain interface between the rotating frame and the stationary frame is located at  $R=1.01$  and the transient sliding mesh interface is adopted for the analysis of unsteady flow due to the rotating jet-wake flow. The calculation time step was the value corresponding to 0.2 deg of the impeller revolution, and the root mean square Courant number was 0.74. Calculation was conducted for 6 revolutions of the impeller. The time averaged statistical value was calculated from the transient results of the last one of the impeller revolutions.

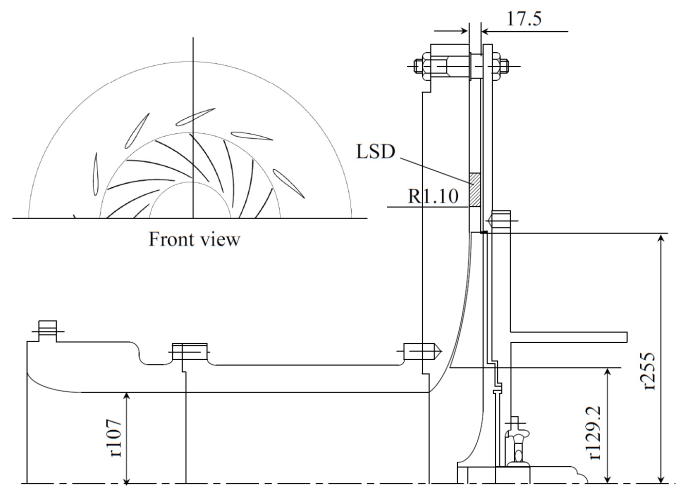


Fig.1 Meridional section of test blower and arrangement of LSD blades

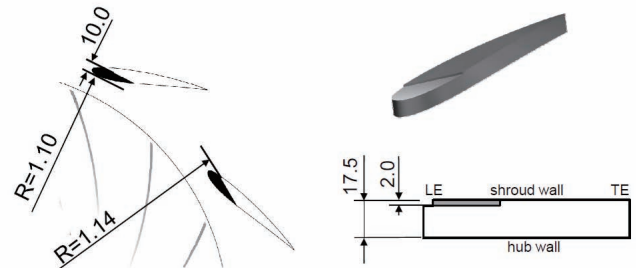


Fig.2 Location of LSD blades and tip-groove configuration

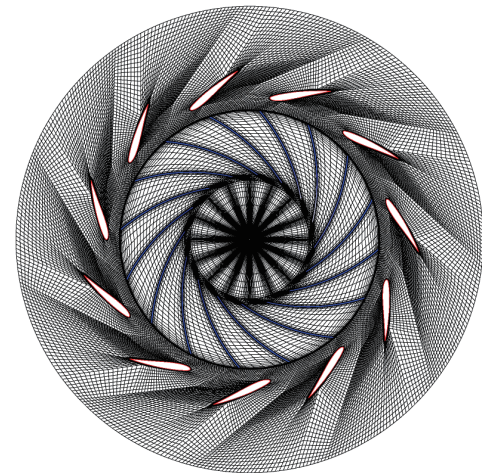


Fig.3 Computational grid for unsteady calculation

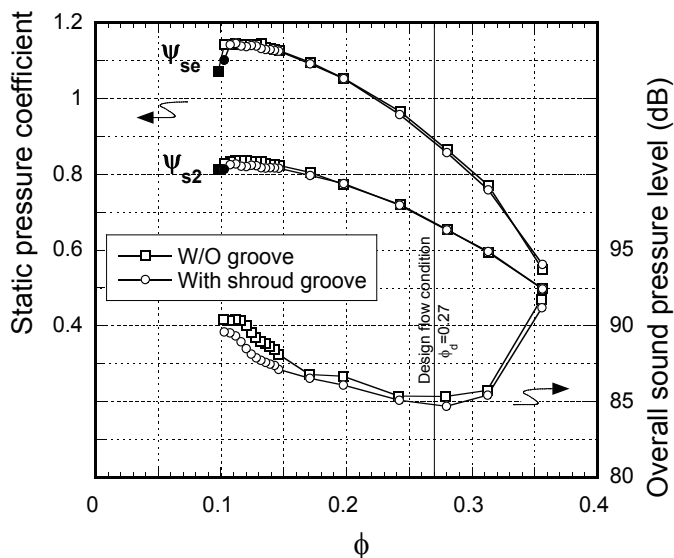


Fig.4 Change in blower characteristics due to tip groove configuration (Exp.)

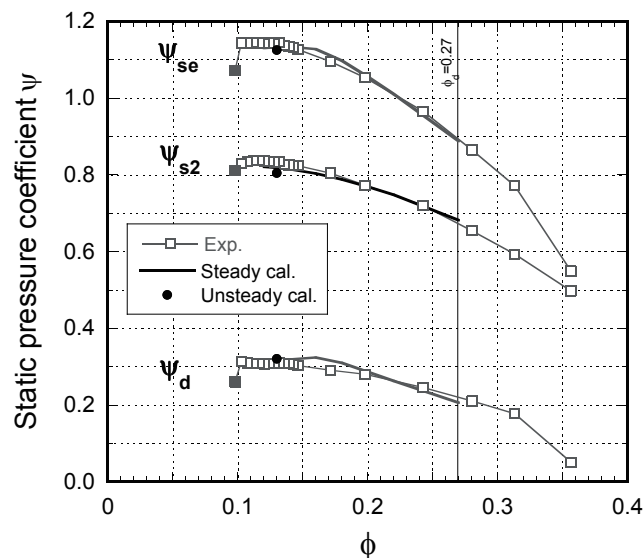


Fig.6 Comparison of static pressure coefficient between experiments and numerical simulation results (w/o groove)

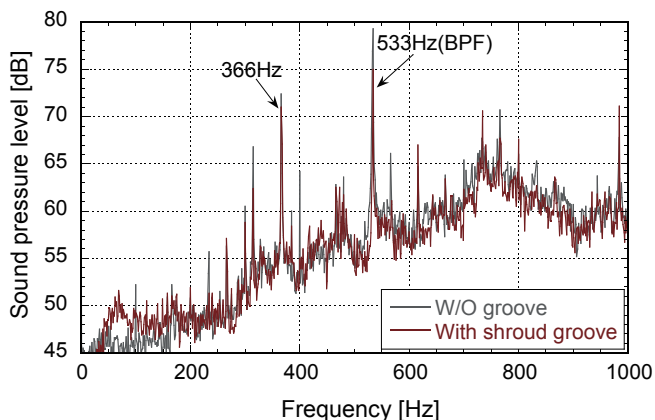


Fig.5 Comparison of frequency spectrum (Exp.,  $\phi=0.13$ )

## RESULTS AND DISCUSSION

### Blower Characteristics

Figure 4 shows the experimental results of the blower characteristics and the overall sound pressure level in comparison between with and without the shroud tip-groove. The abscissa is the discharged flow coefficient  $\phi$ , and the left ordinate is the static pressure coefficient, in which  $\psi_{s2}$  denotes the static pressure coefficient at the impeller exit,  $\psi_{se}$  is the one at the diffuser exit. The solid mark denotes the flow rate at which the diffuser stall appeared. The right ordinate is the overall sound pressure level. In the case with the shroud tip-groove, the overall sound pressure level is decreased without deterioration of the blower characteristics by about 2 dB in maximum at the low flow rate.

Figure 5 shows the frequency power spectra of the sound pressure level measured at the low flow rate of  $\phi=0.13$  in comparison between with and without the shroud tip-groove. The discrete frequency of 533 Hz corresponds to the impeller blade passing frequency (BPF) and that of 366 Hz corresponds to the product of the rotational speed of the impeller and the number of the LSD blades. The discrete frequency of 366 Hz is the characteristic noise which appears under only the low flow rate condition and is based on the circumferentially moving secondary flow at the impeller exit.[8] The BPF sound pressure level decreased markedly by about 5 dB in the cases with the shroud tip-groove compared with the case without groove, the broadband noise between 600-1000 Hz was reduced by about 2 dB, and resulted in the decrease of 2 dB in the overall sound pressure level as shown in Fig.4.

In order to verify the validity of the numerical simulation results, blower characteristics was compared between the experiment and the numerical simulation in Fig.6, where  $\psi_d (= \psi_{se} - \psi_{s2})$  is the static pressure rise in the diffuser. The blower characteristics predicted in both steady and unsteady simulations agree well with the experiment within the experimental accuracy.

### Steady flow analysis

Figure 7 shows the steady simulation result at the low flow rate of  $\phi=0.13$ . The reverse flow zone on the hub side wall is shown as the dark gray region, and the reverse flow zone on the shroud side is shown as the light gray one. In the figure, the representative 3-D streamline which originated in the reverse flow zone is also shown as solid lines. In the case without tip-

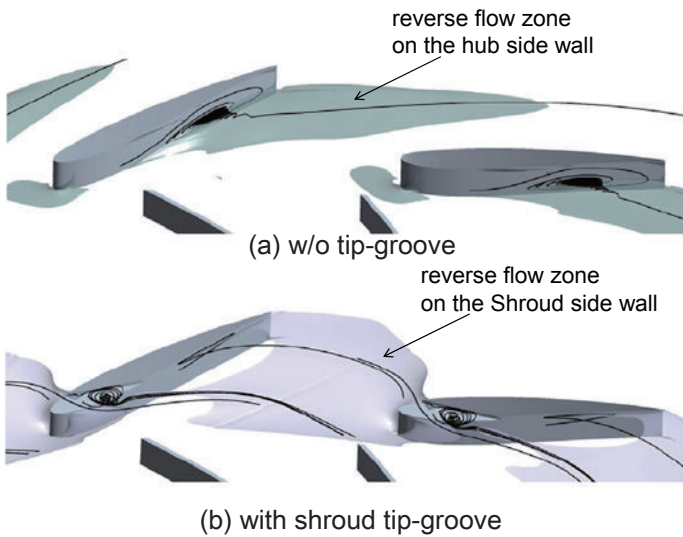


Fig.7 Changes in reverse flow zone and 3-D streamlines due to shroud tip-groove configuration (Steady cal.,  $\phi=0.13$ )

groove as shown in Fig.7(a), the fluid flows downstream out of the suction surface of the LSD blade along the hub wall. On the other hand, in the case with the shroud tip-groove shown in Fig.7(b), the streamlines form into the circumferentially moving secondary flow along the shroud wall toward the impeller exit through the neighboring LSD blade leading edge. It is noticed that the stable and intense vortex is formed in the shroud tip-groove by separation of the circumferentially moving reverse flow.

The meridional velocity contour in the diffuser is compared in Fig.8 between the cases without and with the shroud tip-groove at the low flow rate of  $\phi=0.13$ , where the velocity is averaged circumferentially as the mass-weighted value. The low velocity zone exists at the shroud side upstream of the LSD blade in both cases. In the case without groove, the low velocity zone deviates from the shroud side to the hub side at the downstream of the LSD blade, and this flow behavior seems to be reasonable because of the vorticity component in the meridional plane at the impeller exit. [13] On the other hand, it should be noticed in the case with the shroud tip-groove that the low velocity zone remains at the shroud side from upstream to downstream of the LSD blade, which is due to the secondary flow formed on the shroud wall as shown in Fig.7(b).

### Unsteady flow analysis

**Temporal Variation of Reverse Flow Zone** The unsteady numerical simulation was carried out in order to clarify the influence of the jet-wake flow discharged from the impeller on the flow behavior in the diffuser. The variation of reverse

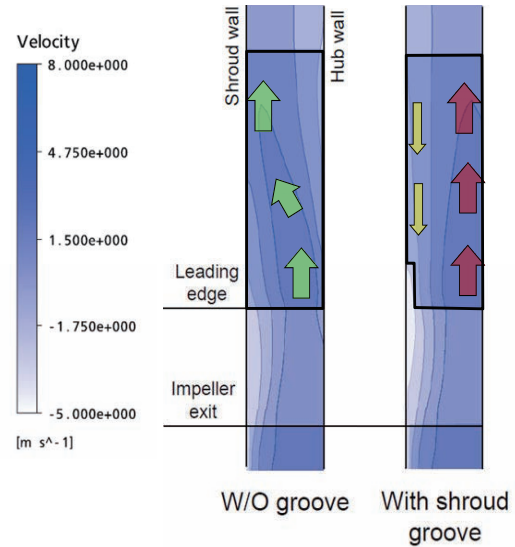


Fig.8 Change in meridional velocity contour in diffuser due to shroud tip-groove configuration (Steady cal.,  $\phi=0.13$ )

flow zone on the diffuser walls are shown in Fig.9, comparing between the cases with and without the shroud tip-groove. The green colored region shows the reverse flow zone on the hub side wall and the gray colored region shows the one on the shroud side wall. Figures 9(a) and (c) show results of the steady simulation and Figs. 9(b) and (d) show the ones of the unsteady simulation. The relative position between the rotating impeller and the LSD blade was changed every 1/4 impeller blade pitch. The reverse flow zone in the case of the unsteady simulation shown in Figs.9(b) and (d) is almost comparable to the one of the steady simulation shown in Figs.9(a) and (c). In Fig.9(b), the reverse flow zone on the hub side wall does not vary even when the relative position of the impeller blade varies because the jet-wake flow decays up to the trailing edge of the LSD blade. It means that the reverse flow zone on the hub side wall is not affected by the jet-wake flow. On the other hand, the reverse flow zone on the shroud side wall in the vaneless space upstream of the LSD varies a little due to the jet-wake flow. In Fig.9(d), the circumferentially moving reverse flow on the shroud wall in the case with the shroud tip-groove is hardly affected by the jet-wake flow because the main flow discharged from the impeller deviates to the hub side and the reverse flow zone exists at the shroud side in the vaneless space upstream of the LSD as shown in the right hand of Fig.8.

**Pressure Fluctuation due to Jet-Wake** Pressure fluctuation on the LSD blade surface due to the jet-wake flow was analyzed based on the unsteady numerical simulation as shown in Fig.10. Four points of the blade surface were selected at the mid span, that is; (a) leading edge, (b) pressure surface at

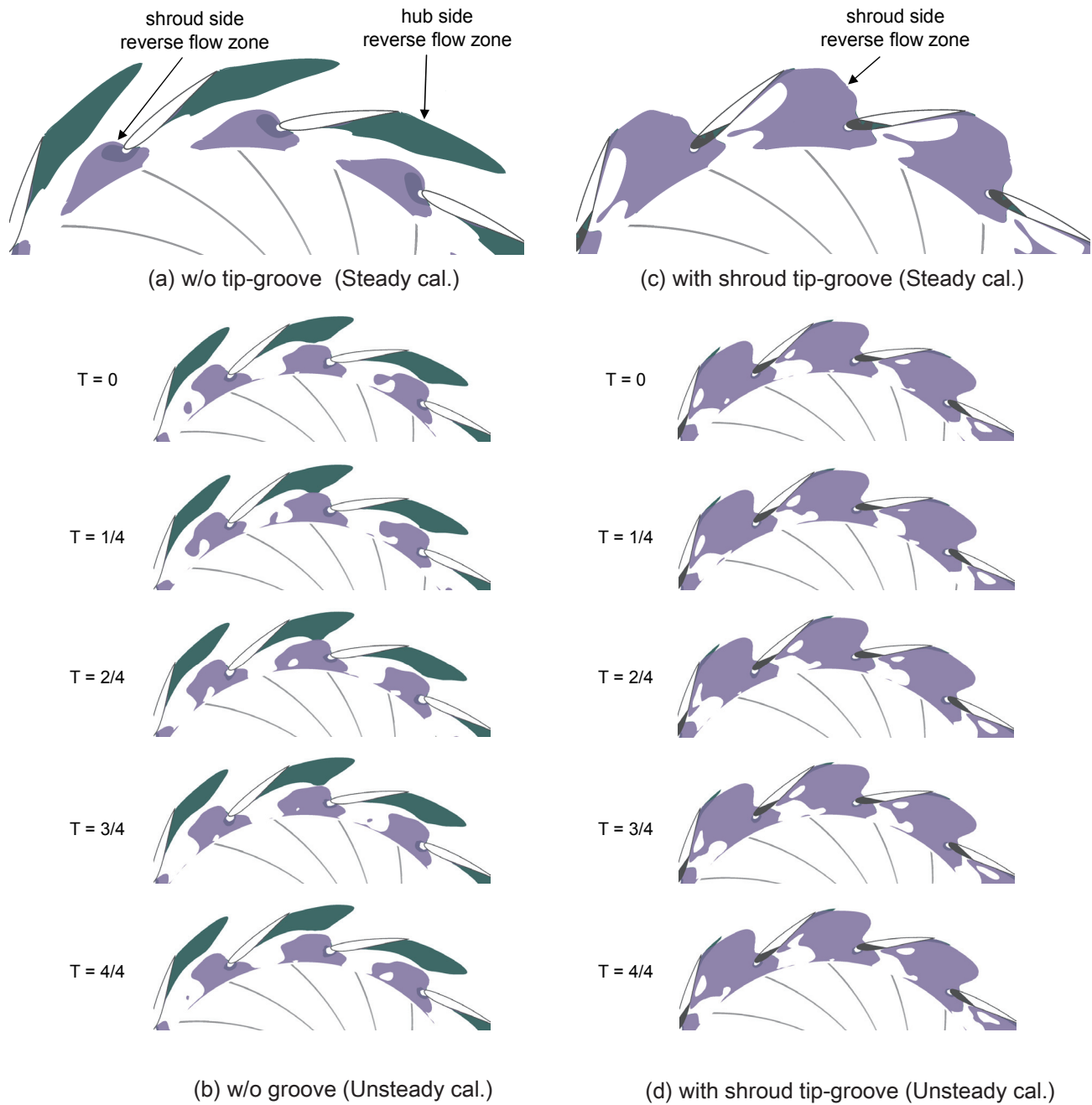
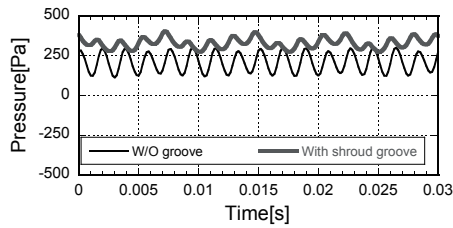
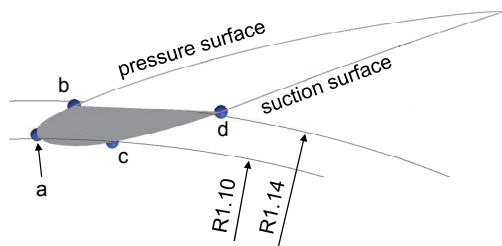


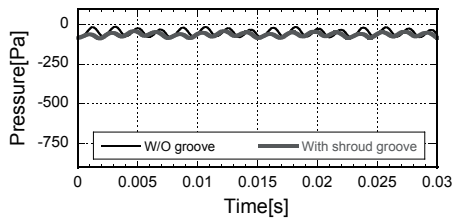
Fig.9 Comparison of reverse flow zone on hub and shroud walls between steady cal. and unsteady cal. ( $\phi=0.13$ )

R=1.14, (c) suction surface at R=1.10 and (d) suction surface at R=1.14, where the abscissa of 0.03 s corresponds to one revolution of the impeller. In Fig.10(a), the periodic pressure fluctuation is clearly seen in the case without groove and its period is equal to the blade passing period, on the other hand, it is not significant in the case with the shroud tip-groove. It is

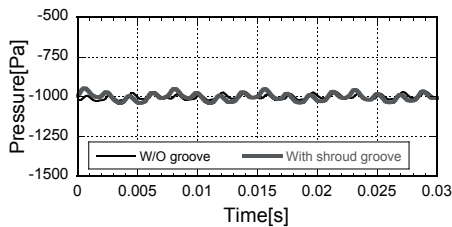
noticed that the influence of the rotating jet-wake flow does not appear due to the circumferentially moving reverse flow from the trailing edge of the LSD blade toward the impeller exit. This is the reason why the BPF noise was reduced by the shroud tip-groove as shown in Fig.5. At the three points except for the leading edge, the amplitude of the pressure fluctuation is small



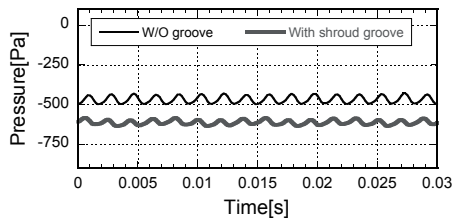
(a) leading edge



(b) pressure surface at R=1.14



(c) suction surface at R=1.10



(d) suction surface at R=1.14

Fig.10 Pressure fluctuation on surface of LSD blade (Unsteady cal.,  $\phi=0.13$ , 50%span)

as shown in Figs.10(b), (c) and (d), and the difference between the cases with and without the shroud tip-groove also small, in other words, the influence of the rotating jet-wake flow on the pressure fluctuation is negligible at the points except for the

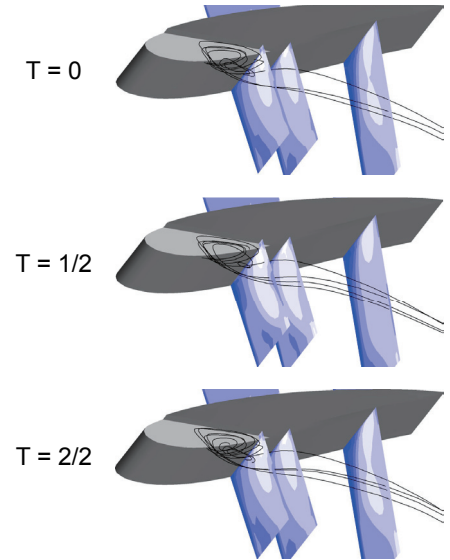
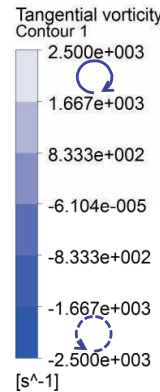


Fig.11 Circumferential vorticity in radial planes near suction surface of LSD blade induced by intense vortex in shroud tip-groove (Unsteady cal.,  $\phi=0.13$ )

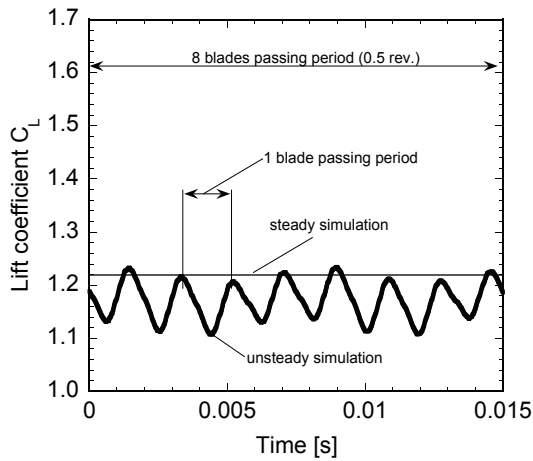
leading edge.

**Temporal Variation of Vortex in Shroud Tip-Groove**

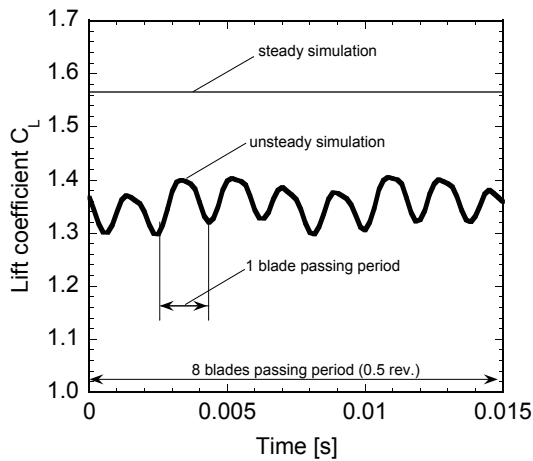
Figure 11 shows temporal variations of the circumferential component of vorticity distribution in the radial planes and the 3-D streamlines flowed out of the shroud tip-groove every time step of 1/2 impeller blade pitch. The intensity of the vortex in the shroud tip-groove and also the clockwise tangential component of vorticity at the shroud side of the suction surface hardly vary when the relative position of the impeller blade varies. In other words, these vortex motions are hardly affected by the rotating jet-wake flow because the reverse flow zone exists at the shroud side upstream of the LSD as mentioned in the previous section. The results based on the unsteady flow analysis are much the same as the ones by the steady flow analysis shown in Fig.7(b).

**Lift Coefficient of LSD Blade**

Figure 12 shows the fluctuation of lift coefficient calculated at the low flow rate of  $\phi=0.13$  with respect to one of the LSD blades. The lift force is normalized by the average dynamic pressure using the vector average velocities calculated at the two sections 5 mm upstream and downstream of the LSD respectively. The periodic fluctuation of the lift coefficient of the LSD blade varies with the blade passing frequency of the rotating impeller in both cases with and without the shroud tip-groove. The magnitude of the fluctuation is nearly equal between the two cases, however, there is a difference in the lift coefficient between the steady and unsteady results, especially it is marked in the case shown in Fig.12(b). The lower value of the lift coefficient in the case of the unsteady simulation seems to be caused by the larger reverse flow zone on the suction surface of the LSD blade as

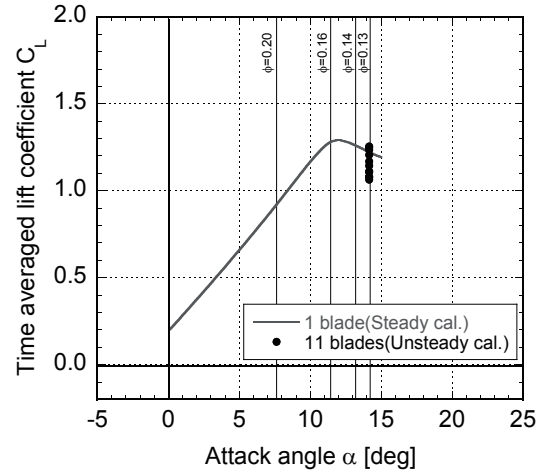


(a) w/o groove

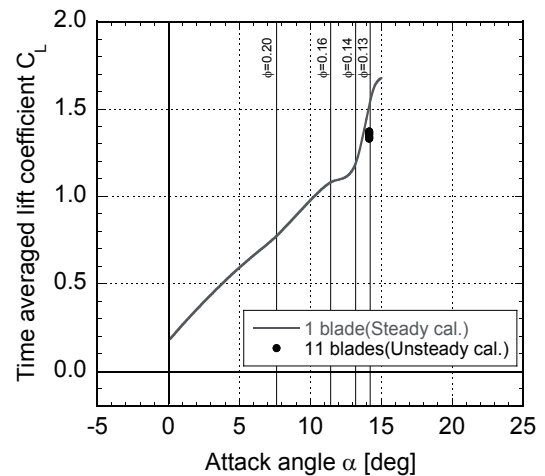


(b) with shroud tip-groove

Fig.12 Fluctuation of lift coefficient  $C_L$  due to jet-wake flow ( $\phi=0.13$ )



(a) w/o groove



(b) with shroud groove

Fig.13 Comparison of lift coefficient  $C_L$  between steady cal. and unsteady cal.

shown in Fig.9(d). It might be caused by a smaller number of calculation grids for one blade passage in the unsteady flow simulation. In the case with the shroud tip-groove, the time averaged lift coefficient by the unsteady simulation and the one by the steady simulation show fairly higher than the one in the case without groove.

Figure 13 shows a comparison of the lift coefficient of the LSD blade in the cases of the steady and unsteady simulations. The abscissa is the angle of attack calculated from the flow rate based on one dimensional analysis. In the case without groove shown in Fig.13(a), the lift coefficient based on the steady simulation decreases remarkably at the angle of attack larger than 12 deg. This is caused by the large reverse flow zone developed on the rear part of suction surface of the LSD blade as shown in Fig.9(a). According to the unsteady simulation, the lift coefficient varies significantly in each LSD blade in the case

without groove as shown by the solid marks in Fig.13(a). This is caused by a small difference in the separation zone on the suction surface of the LSD blade, which is shown by the reverse flow zone in Fig.9(b). On the other hand, in the case with the shroud tip-groove shown in Fig.13(b), the lift coefficient based on the unsteady simulation varies little in each blade. The formation of stable and axisymmetric flow in the diffuser is one of the reason why the high blade loading can be achieved by the shroud tip-groove.

The vortex flowed out of the shroud tip-groove, having the clockwise circumferential component of vorticity, induces the secondary flow from the hub side to the shroud side along the suction surface, then, the flow separation on the suction surface of the LSD blade is suppressed successfully. Further, the low energy fluid accumulated at the shroud side is transported upstream along the shroud wall because the reverse flow zone

exists at the shroud side upstream of the LSD in the case with the shroud tip-groove. In other words, the formation of the circumferentially moving reverse flow suppresses the flow separation on the suction surface, resulting in the high blade loading.

## CONCLUSIONS

In the present paper, the effect of the shroud tip-groove located at the LSD blade leading edge on the blower characteristics and the noise were analyzed by both unsteady and steady flow simulations, comparing with the experimental results as well. The focus was put on the interaction between the rotating jet-wake flow discharged from the impeller exit and the LSD blade. Based on both steady and unsteady flow analyses, the behaviors of the flow separation on the suction surface of the LSD blade and the secondary flow on the side walls were clarified. The following concluding remarks are obtained.

1. In the case with the shroud tip-groove, the stable and intense vortex was formed at low flow rate in both simulations of steady and unsteady analyses.
2. The high blade loading is achieved even under large angle of attack condition by formation of the stable and intense vortex in the shroud tip-groove at low flow rates.
3. In other words, the low energy fluid on the suction surface of the LSD blade is swept up to the shroud wall by the stable and intense vortex formed in the shroud tip-groove, and the low energy fluid accumulated on the shroud wall is transported along the shroud wall moving circumferentially toward the impeller exit through the neighboring LSD blade leading edge.
4. The formation of the stable and intense vortex in the shroud tip-groove is hardly affected by the jet-wake flow discharged from the impeller because the main flow discharged from the impeller exit deviates toward the hub side in the vaneless space upstream of the LSD.
5. In the case with the shroud tip-groove, the flow axisymmetry is preserved in the diffuser even at the low flow rate by the stable vortex formed in the shroud tip-groove, then, the lift coefficient of the LSD blade varies little in each blade, .

## ACKNOWLEDGMENT

This work was financially supported by the Harada Memorial Foundation, and the authors also would like to thank to graduate students of Energy System Laboratory, Nagasaki University for securing the experimental data.

## REFERENCES

- [1] Kang, J. S. and Kang, S. H., 2004, "Steady and unsteady flow phenomena in a channel diffuser of a centrifugal compressor", *JSME Int. J. Series B*, 47, pp.91-100
- [2] Liu, Y., Liu, B. and Lu, L., 2010 "Investigation of Unsteady Impeller-diffuser Interaction in a Transonic Centrifugal Compressor Stage", *ASME GT2010-22737*
- [3] Anish, A. and Sitram, N., 2010 "Steady and transient computations of interaction effects in a centrifugal compressor with different types of diffusers", *ASME GT2010-22913*
- [4] Senoo, Y., Hayami, H. and Ueki, H., 1983, "Low-Solidity Tandem-Cascade Diffusers for Wide-Flow-Range Centrifugal Blowers", *ASME Paper No. 83-GT-3*, pp.1-7
- [5] Hayami, H., Senoo, Y., and Utsunomiya, K., 1990, "Application of Low-Solidity Cascade Diffuser to Transonic Centrifugal Compressor", *Trans. ASME, Journal of Turbomachinery*, Vol.112, No.1, pp.25-29
- [6] Hayami, H., Umemoto, A., 1995, "Effects of Inlet Passage Width Contraction of Low Solidity Cascade Diffusers on Performance of Transonic Centrifugal Compressor", 95-YOKOHAMA-IGTC-15, *Proc. Yokohama International Gas Turbine Congress. II-99-II-102*
- [7] Bonaiuti, D., Arnone, A., Hah, C. and Hayami, H., 2002, "Development of Secondary Flow Field in a Low Solidity Diffuser in a Transonic Centrifugal Compressor Stage", *Proceedings of ASME TURBO EXPO 2002*, GT-2002-30371
- [8] Sakaguchi, D., Ishida, M., Ueki, H., Hayami, H. and Senoo, Y., 2008, "Analysis of Noise Generated by Low Solidity Cascade Diffuser in a Centrifugal Blower", *ASME GT2008-50750*
- [9] Senoo, Y. and Ishida, M., 1975, "Behavior of Severely Asymmetric Flow in a Vaneless Diffuser", *Trans. ASME, Ser.A*, Vol.97, No.3, pp.375-387
- [10] Goto, T., Ohmoto, E., Ohta, Y. and Outa, E., 2009, "Noise Reduction and Surge Margin Improvement Using Tapered Diffuser Vane in a Centrifugal Compressor", *Proc. of the 9th International Symposium on Experimental and Computational Aerothermodynamics of Internal Flows (ISAI9)*, Paper No. 3A-2, pp.1-4
- [11] Zhang, W., Gong, W. Q., Fan, X. H. and Xi, G., 2009, "Experimental Study for the Effect of Vaned Diffuser Leading Edge on the Noise Generated from a Centrifugal Fan", *ASME GT2009-59706*
- [12] Ohta, Y., Goto, T. and Outa, E., 2010, "Unsteady Behavior and Control of Diffuser Leading-edge Vortex in a Centrifugal Compressor", *ASME GT2010-22394*
- [13] Ishida, M., Murakami, T., Sakaguchi, D., Ueki, H., Hayami, H. and Senoo, Y., 2010, "Analysis of Secondary Flow Behavior in Low Solidity Cascade Diffuser of a Centrifugal Blower", *ASME GT2010-2861*